JPE 19-3-16

https://doi.org/10.6113/JPE.2019.19.3.784
ISSN(Print): 1598-2092 / ISSN(Online): 2093-4718

Performance Improvement in Single-Phase Electric Spring Control

Qingsong Wang[*,**], Wujian Zuo[*], Ming Cheng[†], Fujin Deng[*], and Giuseppe Buja[***]

[†,*]School of Electrical Engineering, Southeast University, Nanjing, China
[**]Jiangsu Key Laboratory of Smart Grid Technology and Equipment, Zhenjiang, China
[***]Department of Industrial Engineering, University of Padova, Padova, Italy

Abstract

Two objectives can be pursued simultaneously with the δ control of a single-phase electric spring (ES). These objectives are the stabilization of the voltage across the critical load (CL) of a power system, and the achievement of a specific functionality similar to the pure compensation of reactive power or the correction of the power factor. However, existing control systems implementing the δ control do not cope with non-ideal operating conditions, such as line voltage distortions, and exhibit a somewhat sluggish regulation of the CL voltage. In an effort to improve both the steady-state and transient performances of an ES power system, this paper proposes implementing the δ control by means of a control system built up on the repetitive control and assisted by state feedback with pole assignment. This paper starts by analyzing the dynamics of an ES power system in terms of its poles and zeros. After that, a reduced second-order model of the dynamics is formulated to avoid a notch filter in the pole assignment. A repetitive control for an ES power system is then designed to meet the two above mentioned objectives. Experimental tests carried out on a laboratory setup demonstrate the effectiveness of the proposed control system in significantly improving the ES power system performance, while reaching the two objectives. In particular, the tests outline the large mitigation of harmonics in the CL voltage under line voltage distortions and its fast stabilization action.

Key words: Distributed generation, Electric spring, Grid connected, Microgrids, Pole-assignment, Repetitive control

I. INTRODUCTION

Electric springs (ESs) [1] are a recently proposed technology that helps with the full exploitation of power generated from intermittent renewable energy sources (RESs) [2], [3], especially when they are used to energize a microgrid [4], [5]. In fact, ESs are able to stabilize the voltage across the critical load (CL) of a power system by passing the RES voltage fluctuations to its non-critical load (NCL).

There are three basic topologies of single-phase ESs, which are sequenced as ES-1 [1], ES-2 [6], and ES-3 [7]. All of the ES topologies embed a single-phase current-controlled voltage source inverter (VSI). In ES-1 and ES-2, the VSI output is a capacitor inserted into the NCL branch. The connection of an ES with the NCL is called a smart load (SL) and it is paralleled to the CL at the point of common coupling (PCC). The difference between ES-1 and ES-2 lies in the voltage source of the VSI. It is a capacitor in ES-1 while it is a voltage supply or a battery in ES-2. Unlike ES-1 and ES-2, the ES-3 topology incorporates the concept of active suspension, where the ES is paralleled to the NCL. All three of these topologies are a current topic of research. However, this paper focuses on ES-2. For the sake of convenience, ES-2 will be referred to as ES.

ES power systems are multi-input and multi-output systems. Various strategies have been devised for their control. All of them pursue two objectives. The first one is the key objective of stabilizing the PCC voltage, and the second one is the achievement of a specific functionality such as the pure compensation of reactive power or the correction of the power factor. The δ control strategy, which was proposed in [6], has the distinctive feature of achieving the two objectives by adjusting the phase angle δ of the PCC voltage with respect to the line voltage. The radial-chordal control strategy, which was proposed in [8], decomposes the ES capacitor

Manuscript received Dec. 4, 2018; accepted Feb. 12, 2019
Recommended for publication by Associate Editor Zheng Wang.
[†]Corresponding Author: mcheng@seu.edu.cn
Tel: +86-2583794152, Fax: +86-2583791696, Southeast University
[*]School of Electrical Engineering, Southeast University, China
[**]Jiangsu Key Lab. of Smart Grid Technology and Equipment, China
[***]Department of Industrial Engineering, University of Padova, Italy

voltage into its radial and chordal components. Then it adjusts the radial component to impose the power angle of the SL, and the chordal component to regulate the magnitude of the CL voltage. The active and reactive power control strategy, which was proposed in [9], is aimed at simplifying the control structure of an ES, which makes it more affordable for domestic applications. In addition to the above control strategies, there are many others [10]-[12]. However, none of them has addressed the problem of ES control in the presence of distorted line voltages. The authors of [13] put forward the idea of supplying the ES with a current source. However, this solution is difficult to put into practice and is affected by large losses unless superconducting materials are utilized.

As mentioned above, the δ control has the merit of manipulating only one quantity, i.e. the phase angle δ. Unfortunately, existing control systems implementing the δ control suffer from some shortcomings. In fact, they are arranged around an outer closed-loop with a proportional resonant (PR) regulator to stabilize the CL voltage, and an inner closed-loop with a proportional (P) regulator to control the current delivered by the ES VSI. With such an arrangement, the PR voltage regulator is not able to deal with distorted line voltages and the entire control system exhibits a somewhat sluggish stabilizing action. Considering the merits of the δ control, this paper develops a novel control system that is based on the δ control but able to significantly improve both the steady-state and transient performance of ES power systems.

Repetitive control a type of internal mode control architecture. As such, it succeeds in forcing a controlled system perturbed by distorted variables to track its sinusoidal reference, due to its ability to eliminate harmonic components from control signals [14]-[17]. In return, the dynamics of a system driven by repetitive control are not satisfactory [18]. Pole assignment helps in placing the poles of a system in convenient locations to obtain a desired transient response from a controlled system [19], [20]. In addition, it gives a method for reducing the order of a system to ease the design and setup of its control. In summary, the repetitive control technique, assisted by state feedback with pole assignment, has the potential to substantially improve the performance of ES power systems. This has motivated the development of a control system built on repetitive control to improve the performance of ES power systems. In addition to giving a detailed explanation of the novel control system, this paper contains simulation and experimental results that demonstrate the effectiveness of proposed system. To date, there are no studies reporting on such a control system and/or its experimentation in this field.

This paper is organized as follows. Section II introduces the operating principles of a single-phase ES together with the δ control. Section III formulates and designs both the repetitive control and the state feedback with pole assignment for a δ-controlled ES power system. After listing the data of an ES power system taken as study case, section IV reports the results of simulation tests carried out on the proposed control system to verify its performance. The results confirm that this system outperforms existing control systems, specifically in terms of the suppression of the harmonics of the CL voltage and its fast regulation. Section V corroborates the simulation results with experimental tests. Finally, section VI concludes the paper.

II. Operating Principles of an ES System

A. Circuitry of an ES Power System

Fig. 1(a) illustrates a typical ES topology and the circuitry of a power system integrating the ES. In this figure, the ES is drawn within the dashed line, and comprises a bridge VSI, the filtering inductor L, and the capacitor C inserted into the NCL branch. The ES variables are the capacitor voltage v_{ES}, the VSI output voltage v_i, and the inductor current i_L. The power system variables are as follows: (i) the impedance Z_2 of the CL with a very narrow operating voltage range, (ii) the impedances Z_3 of the NCL with a wide operating voltage range, (iii) the current i_3 through the NCL, (iv) the voltage v_{NC} across the NCL, and (v) the CL voltage v_S. The latter voltage coincides with that of the PCC and is the variable to be stabilized. The voltage v_G and the current i_1 are the line voltage at the RES injection point and the line current, respectively. Meanwhile, R_1 and L_1 are the resistive and inductive components of the line impedance.

B. Existing Implementation of the δ Control

Fig. 1(b) shows a diagram of an existing control system implementing the δ control. The diagram has two nested closed-loops. The outer loop is entered by v_{s_ref}, which represents the sinusoidal reference of the CL voltage, and by its actual value v_S. The magnitude of v_{s_ref} is fixed at the required value whilst its phase lags v_G by the angle δ. The voltage error v_{err} between v_{s_ref} and v_S is fed into the PR regulator to get the reference i_{ref} for the inner loop of the VSI current. The current error between i_{ref} and its actual value i_L is then fed into the P regulator to obtain the voltage reference $v_{\_comp}$ for the VSI output voltage through a limiter. Finally, $v_{\_comp}$ is processed by the PWM generator to deliver the commands of the four VSI switches.

By adjusting the angle δ of v_{s_ref}, two objectives can be pursued for the ES power system, which consist of conveniently managing the power flow within the system and keeping the CL voltage magnitude constant. Once the actual CL voltage is equal to the reference, the two objectives are reached.

Fig. 1(c) shows a vector diagram of an ES power system under a pure reactive power compensation. Moreover, it refers to an ES operating in the inductive mode, which occurs when the CL voltage with no ES action is greater than its rated value. In the opposite case, the ES operates in the

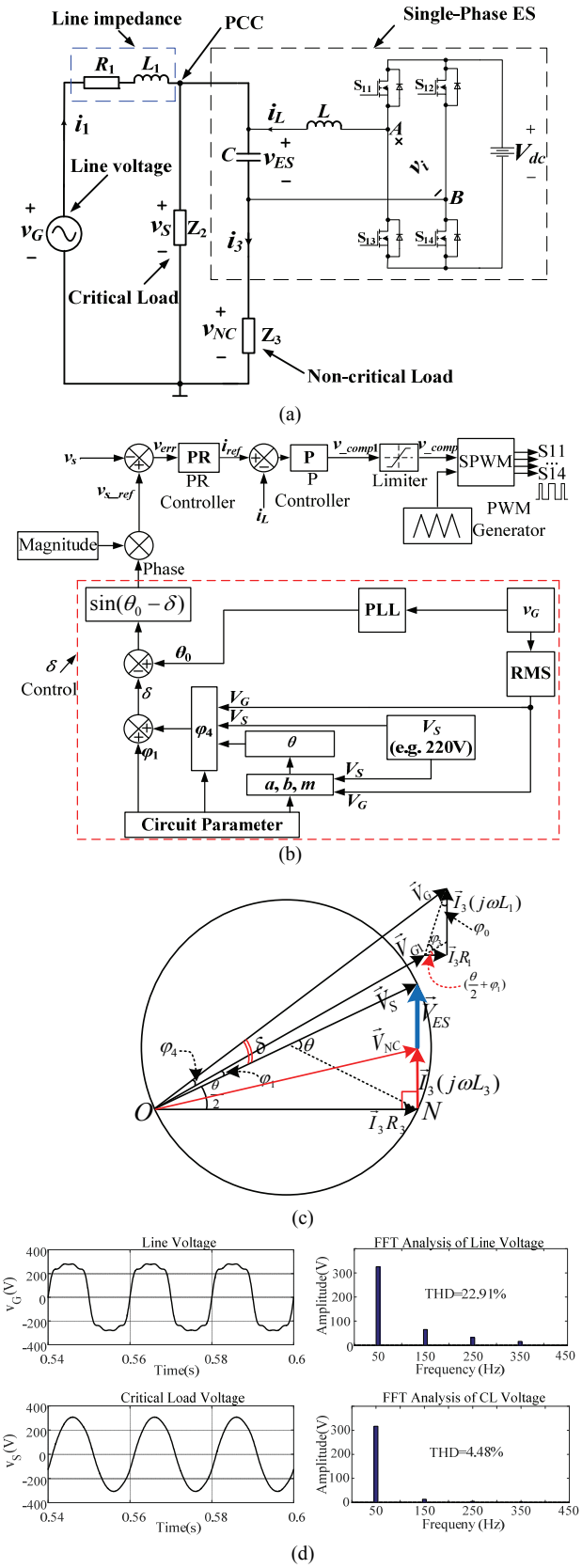

Fig. 1. ES-2 and the δ control. (a) ES power system circuitry. (b) Control diagram. (c) Vector diagram of the δ control in the inductive mode as an example. (d) FFT analysis of the line voltage and CL voltage under distorted line conditions.

capacitive mode and a vector diagram similar to Fig. 1(c) can be traced. The calculation of δ, which can be carried out with the help of the vector diagram in Fig. 1(c), is detailed in [2]. Incidentally, it relies on the prior knowledge of the line impedance.

C. Issues with Existing δ Control

The ES is properly controlled by existing implementations of the δ control under ideal line conditions. However, when v_G is distorted to some extent, the total harmonic distortion (THD) of the CL voltage exceeds the acceptable value, as given in Fig. 1(d). In practice, the gains of the PR regulator should be limited to prevent slightly dampened oscillations of the system. As an example, for the case study in Table I, the gains k_p and k_r of the PR regulator are chosen as 2 and 20, and the gain of the current controller is chosen as 0.5. The resulting THD value of the CL voltage is up to 4.5%, when that of v_G is 23%, which cannot be tolerated by the CL. This is one of the major reasons why there is a need for a better implementation of the δ control.

III. System Modeling and the Proposed Control of an ES System

In this section, an ES power system is modeled. Then the repetitive control and relevant pole assignment for the system are formulated and designed.

A. ES Power System Modeling

The modeling of an ES power system can be simplified by neglecting the DC bus dynamics, if there are any, and assuming that the CL and NCL impedances are of the resistive type. By applying the KCL to the circuit in Fig. 1(a), the following equations can be obtained:

$$i_3 = C\frac{dv_{ES}}{dt} - i_L \tag{1}$$

$$\frac{i_3 R_3 + v_{ES}}{R_2} + i_3 = i_1 \tag{2}$$

Applying the KVL yields:

$$L\frac{di_L}{dt} + v_{ES} = v_i \tag{3}$$

$$L_1\frac{di_1}{dt} + i_1 R_1 + v_{ES} + i_3 R_3 = v_G \tag{4}$$

Solving (1) through (4) yields:

$$\begin{cases} \dfrac{di_L}{dt} = -\dfrac{v_{ES}}{L} + \dfrac{v_i}{L} \\ \dfrac{dv_{ES}}{dt} = \dfrac{i_L}{C} - \dfrac{v_{ES}}{C(R_2+R_3)} + \dfrac{R_2 i_1}{C(R_2+R_3)} \\ \dfrac{di_1}{dt} = -\dfrac{R_2 v_{ES}}{L_1(R_2+R_3)} - \dfrac{(R_1R_2+R_2R_3+R_3R_1)i_1}{L_1(R_2+R_3)} + \dfrac{v_G}{L_1} \end{cases} \tag{5}$$

Applying the KVL also yields:

$$v_S = v_{ES} + i_3 R_3 \tag{6}$$

$$v_S = v_G - i_1 R_1 - L_1 \frac{di_1}{dt} \tag{7}$$

The quantities i_L, v_{ES} and i are chosen as the state variables of the ES power system. The system has one output and two inputs, where one of them is the line voltage. This is not within the action of the control system. As a result, it acts as a disturbance input on the ES power system. Then (5) can be written in the following form:

$$\begin{cases} \dot{x} = A_c x + B_{c1} v_i + B_{c2} v_g \\ y = C_c x \end{cases} \tag{8}$$

where:

$$x = \begin{bmatrix} i_L & v_{\mathrm{ES}} & i_1 \end{bmatrix}^{\mathrm{T}}, \quad y = v_S$$

$$A_c = \begin{bmatrix} 0 & -\frac{1}{L} & 0 \\ \frac{1}{C} & -\frac{1}{C(R_2+R_3)} & \frac{R_2}{C(R_2+R_3)} \\ 0 & -\frac{R_2}{L_1(R_2+R_3)} & -\frac{R_1R_2+R_2R_3+R_3R_1}{L_1(R_2+R_3)} \end{bmatrix}$$

$$B_{c1} = \begin{bmatrix} 0 \\ 0 \\ \frac{1}{L_1} \end{bmatrix}, B_{c2} = \begin{bmatrix} \frac{1}{L} \\ 0 \\ 0 \end{bmatrix}, C_c = \begin{bmatrix} 0 & \frac{R_2}{R_2+R_3} & \frac{R_2R_3}{R_2+R_3} \end{bmatrix}.$$

B. Control System Diagram

A diagram of the novel control system for an ES power system is shown in Fig. 2, where d is the disturbing term. In addition to the δ calculation block, the diagram contains the blocks of the repetitive control and the state feedback with pole assignment. Their formulation and the design of the relevant algorithms are presented below, starting with the pole assignment.

C. Pole Assignment Design

State feedback with pole assignment is an effective method to speed up the dynamics of a controlled system. Since line voltage is a disturbance, it is disregarded in assigning the system poles due to the fact that it does not affect the eigenvalues of the system.

Let the control signal v_i of a system be given by:

$$v_i = v_{i\_ref} - Kx \tag{9}$$

where v_{i_ref} denotes the reference signal, and K is the feedback gain matrix, which is $[k_1, k_2, k_3]$ for a system with three state-variables. Then the state equation of the controlled system can be rewritten as:

$$\dot{x} = (A_c - B_{c1})x + B_{c1} v_{i\_ref} \tag{10}$$

The new poles of the system are given by the eigenvalues

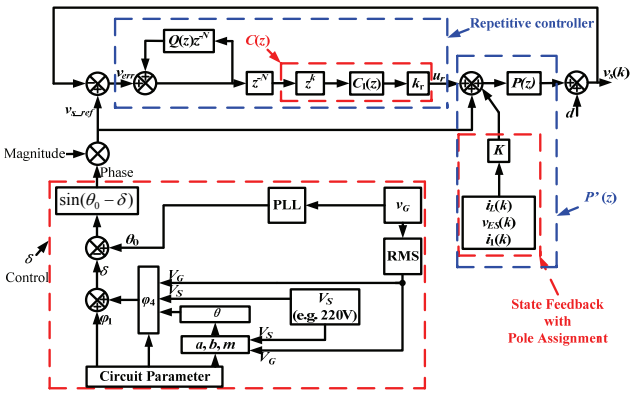

Fig. 2. Repetitive control diagram implementing the δ control.

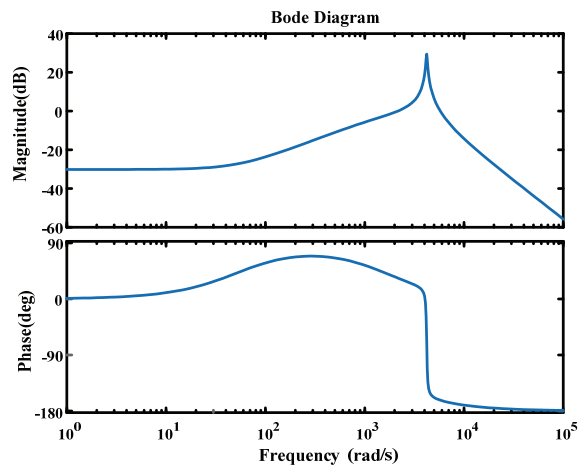

(a)

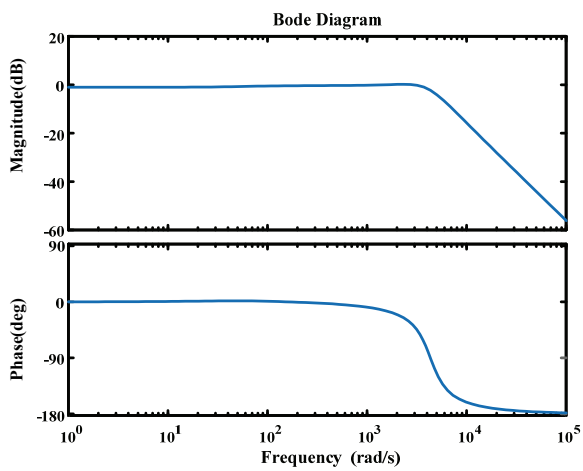

(b)

Fig. 3. Bode diagram of an ES power system. (a) Without pole assignment. (b) With pole assignment.

of (A-BK), and can be assigned arbitrarily with a proper selection of the feedback gains.

For the study case in Section VI, Figs. 3(a) and (b) plot Bode diagrams for the ES power system of the case study without and with pole assignment. From the two figures, it can be seen that the pole assignment favorably reshapes the Bode diagram by flattening the curves of both the magnitude

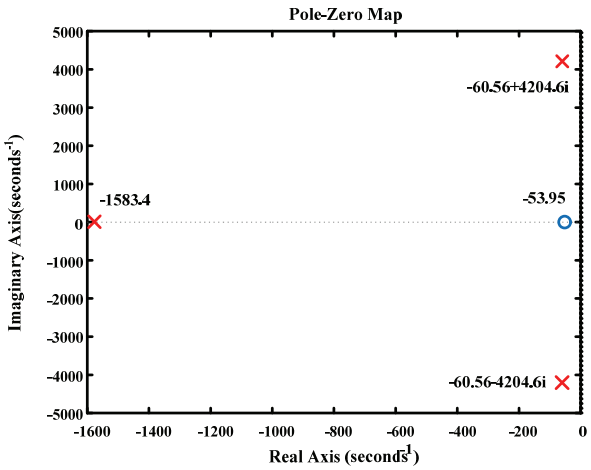

Fig. 4. Pole-Zero maps of an ES power system.

and the phase. With the help of the Pole-Zero map in Fig. 4, the effects of the pole assignment can be clearly seen. While the original ES power system has one zero and three poles, the pole assignment cancels out the zero and reassigns the pair of predominant poles far from the imaginary axis. The two combined actions dampen the system and speed up its response by notably shortening the settling time. Moreover, by neglecting the pole with a large negative real part, the ES power system becomes the second-order type, which facilitates the repetitive control design.

D. Repetitive Controller Design

Although pole assignment enhances the transient performance of an ES power system, it does not guarantee desirable steady-state performance. Thus, it is supplemented by repetitive control, as explained below.

Let the control of an ES power system be executed by digital devices. The design of the control requires a discretized model of the ES power system. By assuming that the sampling period is equal to the switching period of the VSI and that the discrete model is obtained by the ZOH method, the discrete state equation of the ES power system after the insertion of the state feedback is obtained as follows:

$$\begin{cases} x(k+1) = (A\text{-}B_1\mathrm{K})x(k) + B_1 v_i(k) + B_2 v_g(k) \\ y(k+1) = C_c x(k) \end{cases} \tag{11}$$

where:

$$A = e^{AcT},\ \mathrm{B}_1 = A_c^{-1}(e^{AcT} - 1)B_{c1},\ \mathrm{B}_2 = A_c^{-1}(e^{AcT} - 1)B_{c2}.$$

The concept of repetitive control is well documented in the literature. Here, a repetitive control of the plug-in type is used, as shown in Fig. 2. It relies on adding the term u_r to the voltage reference v_{s_ref} to accomplish a repetitive correction of the system. In this case, the term u_r is obtained by manipulating the voltage error v_{err}. Hereafter, the formulation and design of the repetitive control are carried out in the z-domain.

The key element of repetitive control is the internal model $1/(1\text{-}Q(z)z^{-N})$, which represents the transfer function of the inner positive feedback. This function is composed of two quantities, i.e. the term z^{-N}, which postpones the control signal by N sampling times; and the function $Q(z)$, which can be either a low-pass filter or a constant smaller than 1. This function helps reject disturbances while sacrificing the steady error. Then its design is a tradeoff between the robustness and steady-state accuracy of the controlled system.

The output of the internal model is then processed by the compensation unit $z^{-N}\ C(z)$ to get u_r. In turn, z^{-N} makes z^k be achieved by DSP. In addition, $C(z)$ consists of the time-advance block z^k; the cascade compensator $C_1(z)$, which is used to expand the frequency bandwidth of the system; and the control gain k_r.

The main tasks in designing a repetitive control are to synthesize an appropriate transfer function for $C_1\ (z)$ and an appropriate value of k for the block z^k. Since state feedback with pole assignment is designed to eliminate the peak resonance of an ES power system, a second-order low-pass transfer function for $C_1\ (z)$ ensures sufficient filtering of the control signal in the forward path, which gives the system satisfactory dynamic behavior. The block z^k counteracts the delay introduced by the term z^{-N} in the inner positive feedback. In addition, through the parameter k, it directly impacts the stability margin, the convergence speed of the error, and the harmonic suppression of the controlled system.

From Fig. 2, the following can be obtained:

$$\begin{aligned} e(z) = &\frac{(1-P'(z))(z^N - Q(z))}{z^N - (Q(z) - z^k k_r C_1(z)P'(z))} v_{s\_ref}(z) \\ &+ \frac{Q(z) - z^N}{z^N - (Q(z) - z^k k_r C_1(z)P'(z))} d(z) \end{aligned} \tag{12}$$

where $P(z)$ and $P'(z)$ are the state matrixes of the ES-2 power system after and before the insertion of state feedback with pole assignment. According to the small gain theorem, a sufficient condition for stability of the system is as follows:

$$\left|\mathrm{H}(e^{j\omega T})\right| < 1 \tag{13}$$

where $H(e^{j\omega T}) = Q(e^{j\omega T}) - e^{j\omega kT} k_r C_1(e^{j\omega T})P'(e^{j\omega T})$, ω=[0, π/T] and T is the sample time. This means that if ω is varied from 0 to π/T and the end point of the vector $e^{j\omega kT}K_rC_1(e^{j\omega T})P'(e^{j\omega T})$ does not exceed the unity circle centered at the end point of $Q(e^{j\omega T})$, the repetitive control system is regarded as sufficiently stable.

The design process of the repetitive control proceeds is as follows (the relevant Bode diagram is plotted in Fig. 5).

(1) Model the ES power system including the state feedback. This task is mainly concerned with the pole assignment of the feedback system.
(2) Select the coefficients of the second-order low-pass filter $C_1(z)$.
(3) Select the constant k of the time-advance block.

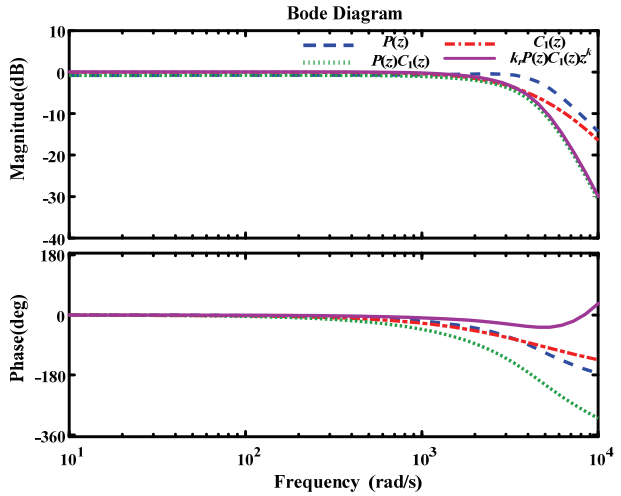

Fig. 5. Bode diagrams in the design process of the repetitive control.

(4) Select $Q(z)$ and k_r to obtain the best balance between the stability margin and harmonic suppression. Here, for the sake of simplicity, $Q(z)$ is selected to be a constant, and is set to 0.95.

E. Full-Order Observer Design

To work around the delay introduced by the sampling time operation of an ES power system, it is useful to predict the control input one sampling period ahead and enter the system with it. The prediction can be appropriately estimated by means of a full-order state observer. The observer equations can be expressed as:

$$\begin{cases} \hat{x}(k+1) = (A - HC_c)x(k) + Bu(k) + Hy(k) \\ \hat{y}(k) = C_c\hat{x}(k) \end{cases} \quad (14)$$

where $B = \begin{bmatrix} B_1 & B_2 \end{bmatrix}$, $u = \begin{bmatrix} v_i & v_g \end{bmatrix}^T$, and H is the observer gain matrix, where it is made of only one element. By (14), the observer error can be written as:

$$e(k+1) = x(k+1) - \hat{x}(k+1) = (A - HC_c)(x(k) - \hat{x}(k)) \quad (15)$$

The poles of the observer can be arbitrarily placed by selecting a suitable gain of H. A practical rule is to place the real part of the poles of a state observer 2 to 3 times higher than that of the poles of the system to ensure that the error of the observer vanishes as quickly as possible.

IV. Simulations and Discussions

To verify the performance of the developed control system implementing the δ control for an ES power system, simulations are conducted in MATLAB/Simulink for a case study. The data for this study is listed in Table I. It should be pointed out that the value of the line impedance was enlarged in order to make the control performance more apparent. Two simulation codes have been written, the first one to execute pure reactive power compensation and the second one for PFC functionality. The control system objectives are finalized by regulating the CL voltage at 110V. In addition, the pure reactive power compensation is achieved by imposing the phase angle between ES current and voltage at 90°, and the PFC functionality is achieved by imposing the line current in phase to the voltage v_G.

TABLE I
Data of the ES Power System Case Study

Items	Values
PCC voltage (V_S)	110V
DC bus voltage (V_{dc})	200V
Line resistance (R_1)	1.64Ω
Line inductance (L_1)	30.4mH
Critical load (Z_2)	1600Ω
Non-critical load (Z_3)	51Ω
Inductance of ES filter (L)	2.3mH
Capacitance of ES filter (C)	26μF
Switching frequency (f)	20kHz

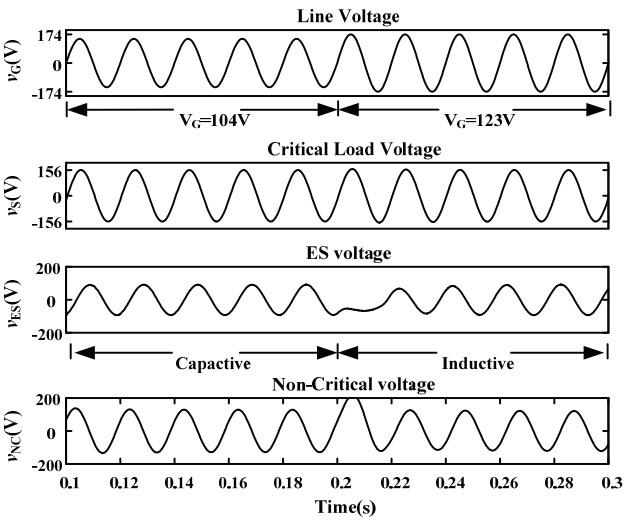

Fig. 6. Waveforms obtained with the developed control system under pure reactive power compensation for ideal grid conditions.

A. Pure Reactive Power Compensation

For the pure power compensation, simulations have been carried out in two stages. The first stage is under ideal line conditions and the second stage is under line voltage distortion.

1) Ideal Line Conditions: Fig. 6 shows waveforms obtained under ideal line conditions with the developed control system. As in [6], the values of 104V and 123V are selected for the magnitude of v_G to reproduce the capacitive and inductive operation modes of the ES, respectively. This figure presents the line voltage, the CL voltage, the ES voltage and the NCL voltage. These waveforms give the system behavior in the two modes. From 0.1 to 0.2s, the magnitude of v_G is set to 104V and the ES current, which is in phase with the NCL

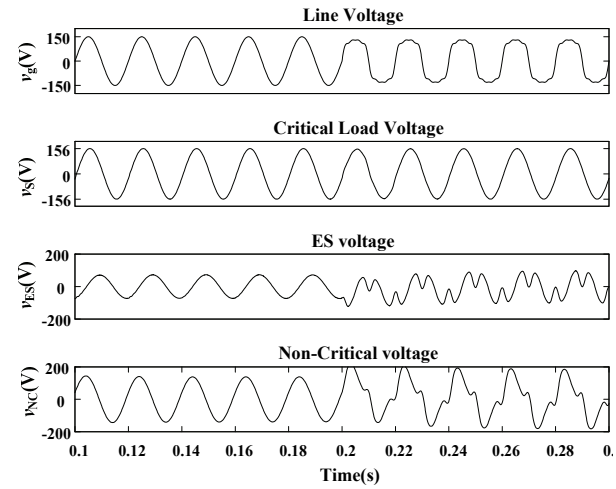

(a)

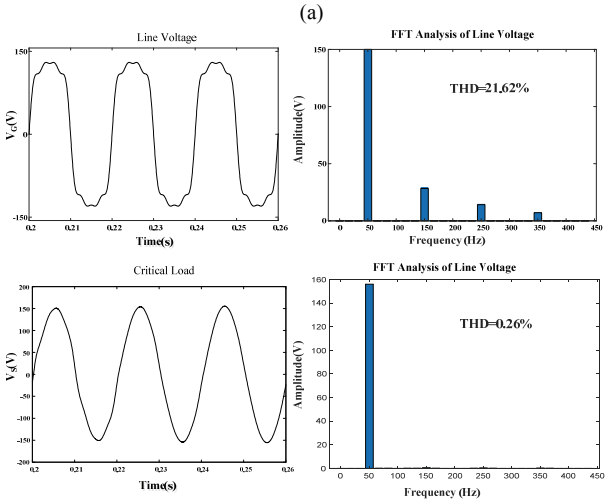

(b)

Fig. 7. Waveforms obtained with the developed control system under reactive power compensation. (a) Comparison between the ideal and distorted line conditions. (b) FFT analysis of the line and CL voltages under distorted line conditions.

voltage, leads the ES voltage by 90°. This means that the ES operates in the capacitive mode. From 0.2 to 0.3s, the magnitude of v_G is set to 123V and the ES current lags the ES voltage by 90° after a transition interval of about 0.05s. This means that the ES operates in the inductive mode. The waveforms in Fig. 6 also emphasize the tight regulation of the CL voltage, which is a sinewave with an RMS value close to 110V.

The results above validate the effectiveness of the proposed control system in stabilizing the CL voltage for ideal line conditions while compensating for the reactive power absorbed by the power system.

2) Distorted Line Voltage: The simulations here are conducted by shaping the line voltage as follows. From 0 to 0.3s, the nominal value of v_G is set to 106V without any distortion. From 0.3s to 0.6s, the 3rd, 5th and 7th harmonics of voltage with magnitudes of 20V, 10V and 5V are added to the fundamental component. As a result, the THD value of v_G

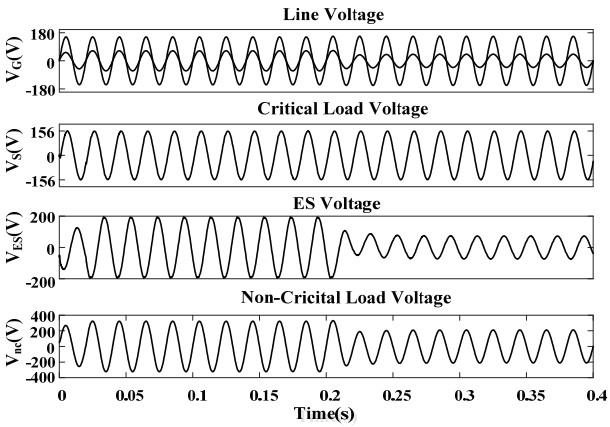

Fig. 8. Waveforms obtained with the developed control system under PFC functionality.

is about 22%, which is the same as the value in Fig. 2(c). Fig. 7(a) shows waveforms before and after a line voltage distortion. Before 0.2s, the ES operates in the capacitive mode and the ES and CL voltages are sinusoidal. After 0.3, the waveforms show that the distortion of the line voltage is passed to the NCL voltage. It can also be seen that the CL voltage stays properly regulated during the entire simulation time. In turn, Fig. 7(b) shows that the THD value of the CL voltage is kept at 0.26%, which is much smaller than the THD value obtained with the existing control system as shown in Fig. 1(d).

B. PFC Functionality

For the PFC functionality, the same simulation code as above is used. The only difference is the calculation of the angle δ, which is executed as in [6] and is aimed at bringing the line power factor to 1. The simulation time is divided into two intervals. In the first interval, which goes from 0 to 0.2s, the magnitude of v_G is set to 108V. In the second interval, which goes from 0.2s to 0.4s, the magnitude of v_G is set to 112V.

Fig. 8 shows waveforms obtained with the developed control system under ideal line conditions. In this figure, four quantities are recorded. In the first channel, the line voltage is recorder together with the line current to highlight the achievement of the PFC functionality. It can be seen from the waveforms that the two quantities cross the zero point at the same time. This means that the line current is in phase with the line voltage and that this condition is met even when the ES operating mode changes from capacitive to inductive. The CL voltage is recorded in the second channel, and the resulting waveform shows that it is well regulated at 110V. The ES and NCL voltages are recorded in the 3rd and 4th channels, respectively. By remembering that the NCL is of the resistive type, an inspection of the waveforms in the latter two channels shows that the two quantities are not in quadrature. For instance, at 0.105s, when the magnitude of v_G is 108V, the ES current leads the ES voltage by more than 90°. This means that the ES provides some active power to the power system. At 0.365s, when the magnitude of v_G is 112V, the ES current

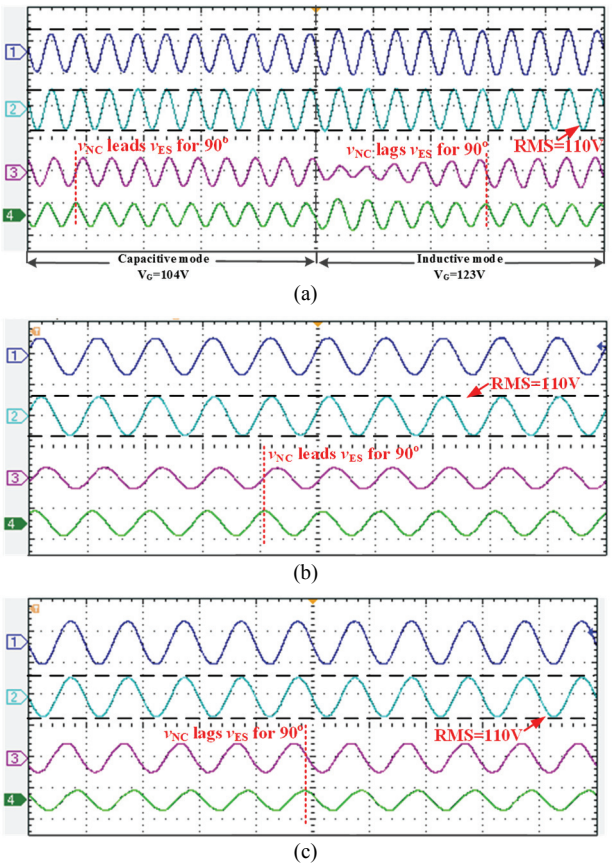

Fig. 9. Measured voltage waveforms for the ES power system without line voltage distortion (250 V/div, 20 ms/div). Ch1: line voltage; Ch2: CL voltage; Ch3: ES voltage; Ch4: NCL voltage. (a) Transient response from the capacitive to inductive mode. (b) Capacitive mode @ V_G=104 V. (c) Inductive mode @ V_G=123V.

leads the ES voltage by less than 90°. This means that the ES absorbs some active power from the power system.

These outcomes make it possible to state that the simulation results validate the effectiveness of the proposed control system in stabilizing the CL voltage while correcting for the power factor of the line.

V. Experiments

In this section, measurements are detected from an experimental setup made of an ES power system with the same data as in Table I and driven by the developed control system. The setup has been subjected to the same tests carried out by the simulations.

A. Pure Reactive Power Compensation

1) Ideal Line Conditions: The waveforms in Fig. 9 are measured under ideal line conditions and report the steady-state and transient operations of the ES power system. Four quantities are recorded in the subfigures, where the quantities are the same as those in Fig. 6. Fig. 9(a) shows the transients of the quantities after a change of the operating mode from

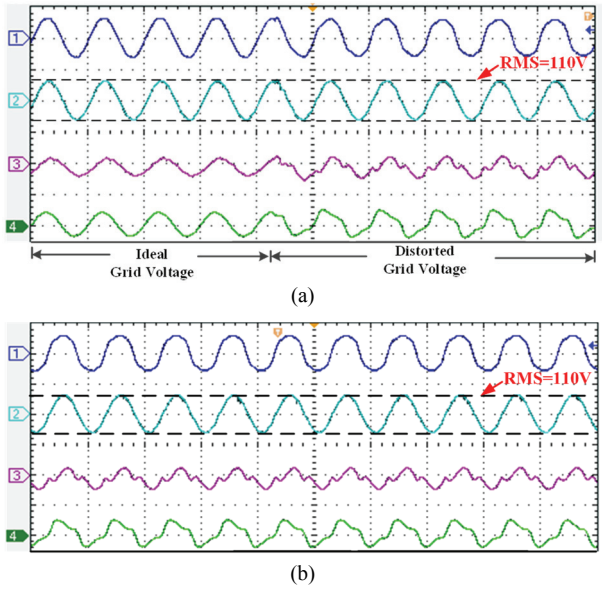

Fig. 10. Measured voltage waveforms for different line voltage conditions (250 V/div, 20 ms/div). Ch1: line voltage; Ch2: CL voltage; Ch3: ES voltage; Ch4: NCL voltage. (a) Transition from an ideal to a distorted line voltage. (b) Steady-state waveforms under line voltage distortion.

capacitive to inductive. For up to half of the recorded time interval, the line voltage is set to 104V. As required, the CL voltage is regulated at 110V and the ES current, which is in phase with the NCL voltage, leads the ES voltage by 90°. After that, the line voltage is stepped up to 123V. The CL voltage remains steady while the ES current starts to lag the ES voltage to obtain a shift of 90° at the transient completion. For the sake of convenience, the two operating modes are displayed separately at steady state in Figs. 9(b) and 9(c).

2) Distorted Line Voltage: Waveforms measured when the ES operates under line voltage distortion are shown in Fig. 10. At the beginning of the experiment, the voltage v_G is sinusoidal with its magnitude set to a nominal value of 106V. It is then subjected to the fundamental components of 3rd, 5th and 7th order harmonics with magnitudes of 20V, 10V and 5V, respectively. Fig. 10(a) shows that at the beginning of the experiment all of the detected voltages are sinusoidal, with the ES operating in the capacitive mode.

After the harmonics have been added, it can be clearly seen from the shapes of the waveforms that the distortion of the line voltage is passed to the NCL. These measurements outline once again that the CL voltage is well regulated under line voltage distortion.

B. PFC Mode

Measured waveforms for the ES power system under the PFC functionality are shown in Fig. 11. Here, three channels are displayed where the line voltage and current are recorded in the first channel, the CL voltage is recorded in the second channel and the ES voltage is recorded in the third channel.

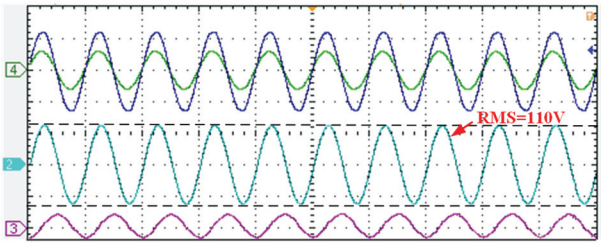

Fig. 11. Measured voltage waveforms for the ES power system under PFC functionality (20ms/div). Ch1: line voltage (125V/div) and line current (10A/div); Ch2: CL voltage (125V/div); Ch3: ES voltage (125V/div).

The experimental results show that the line voltage and current have the same zero crossing points. This means that the two quantities are in phase, as requested by the PFC functionality. In addition, the waveform of the CL voltage demonstrates that it is regulated at 110V, while the waveform of the ES voltage demonstrates that it is not in quadrature with the ES current (note that the ES current is in phase with the line current because both CL and NCL are of the resistive type). This reveals an exchange of active power between the ES and the power system.

Considering the outcomes detected from the ES power system driven by the developed control system when the δ control incorporates pure reactive power compensation and PFC functionality, the findings obtained by the simulation are fully corroborated by the experiments.

VI. Conclusions

In this paper, a new control strategy implementing the δ control was proposed for an ES power system to improve the performances in both the steady and transient states. When compared to the performance exhibited with existing control systems. The proposed control system implements a repetitive control assisted by a state feedback with pole assignment. The performance improvement is concerned with the mitigation of voltage distortion across the CL in the presence of a distorted line, and the reduction of the settling time of the CL voltage at the regulated value after a fluctuation of the line voltage.

Specifically, this paper has provided the formulation and design of all the control tools used to arrange the control system: repetitive control, state feedback and pole assignment. Their combined action is used to properly control an ES-power system. In terms of the δ control, it has been determined to meet the typical functionalities of pure reactive power compensation and PFC. Simulation and experimental results have demonstrated that the proposed control system is able to accurately regulate the CL voltage while precisely executing the required functionality. Then they validate the effectiveness of the control system in achieving the sought for performance improvement of an ES power system.

Acknowledgment

This work was supported by the Natural Science Foundation of Jiangsu Province under project BK20170675, and by the National Natural Science Foundation of China under project 51877040.

References

[1] S. Y. R. Hui, C. K. Lee, and F. Wu, "Electric springs – A new smart grid technology," *IEEE Trans. Smart Grid*, Vol. 3, No. 3, pp. 1552-1561, Sep. 2012.

[2] M. Cheng and Y. Zhu, "The state of the art of wind energy conversion systems and technologies: A review," *Energy Convers. Manag.*, Vol. 88, pp. 332-347, Dec. 2014.

[3] Z. Gong, X. Wu, P. Dai, and R. Zhu, "Modulated model predictive control for MMC-based active front-end rectifiers under unbalanced grid conditions," *IEEE Trans. Ind. Electron.*, Vol. 66, No. 3, pp. 2398-2409, Mar. 2019.

[4] J. M. Guerrero, J. C. Vasquez, J. Matas, L. G. de Vicuna, and M. Castilla, "Hierarchical control of droop-controlled AC and DC microgrids – A general approach toward standardization," *IEEE Trans. Ind. Electron.*, Vol. 58, No. 1, pp. 158-172, Jan. 2011.

[5] Q. Sun, J. Zhou, J. M. Guerrero, and H. Zhang, "Hybrid three-phase/single-phase microgrid architecture with power management capabilities," *IEEE Trans. Power Electron.*, Vol. 30, No. 10, pp. 5964-5977, Oct. 2015.

[6] Q. Wang, M. Cheng, Z. Chen, and Z. Wang, "Steady-state analysis of electric springs with a novel δ control," *IEEE Trans. Power Electron.*, Vol. 30, No. 12, pp. 7159-7169, Dec. 2015.

[7] C. K. Lee and S. Y. R. Hui, "Input AC voltage control bi-directional power converters," U.S. Patent 13/907, 350, May 31, 2013.

[8] K. T. Mok, S. C. Tan, and S. Y. R. Hui, "Decoupled power angle and voltage control of electric springs," *IEEE Trans. Power Electron.*, Vol. 31, No. 2, pp. 1216-1229, Feb. 2016.

[9] Q. Wang, M. Cheng, Y. Jiang, W. Zuo, and G. Buja, "A simple active and reactive power control for applications of single-phase electric springs," *IEEE Trans. Ind. Electron.*, Vol. 65, No. 8, pp. 6291-6300, Aug. 2018.

[10] X. Chen, Y. Hou, S. C. Tan, C. K. Lee, and S. Y. R. Hui, "Mitigating voltage and frequency fluctuation in microgrids using electric springs," *IEEE Trans. Smart Grid*, Vol. 6, No. 2, pp. 508-515, Mar. 2015.

[11] S. Yan, S. C. Tan, C. K. Lee, and S. Y. R. Hui, "Electric springs for reducing power imbalance in three-phase power systems," *IEEE Trans. Power Electron.*, Vol. 30, No. 7, pp. 3601-3609, Jul. 2015.

[12] Q. Wang, D. Zha, F. Deng, M. Cheng, and G. Buja, "A topology of DC electric springs for DC household applications," *IET Power Electron.*, 2019, in press, doi: 10.1049/iet-pel.2018.6237.

[13] Q. Wang, M. Cheng, and Y. Jiang, "Harmonics suppression for critical loads using electric springs with current-source inverters," *IEEE J. Emerg. Sel. Topics Power Electron.*, Vol. 4, No. 4, pp. 1362-1369, Dec. 2016.

[14] K. Zhou and D. Wang, "Digital repetitive controlled three-phase PWM rectifier," *IEEE Trans. Power Electron.*, Vol. 18, No. 1, pp. 309-316, Jan. 2003.

[15] Y. Yang and K. Zhou, "Analysis and mitigation of dead-time harmonics in the single-phase full-bridge PWM converter with repetitive controllers," *IEEE Trans. Ind. Appl.*, Vol. 54, No. 5, pp. 5343-5354, April. 2018.
[16] N. Marati and D. Prasad, "A modified feedback scheme suitable for repetitive control of inverter with nonlinear load," *IEEE Trans. Power Electron.*, Vol. 33, No. 3, pp. 2588-2600, Mar. 2018.
[17] K. Zhou, K. S. Low, D. Wang, F. Luo, B. Zhang, and Y. Wang, "Zero-phase odd-harmonic repetitive controller for a single-phase PWM inverter," *IEEE Trans. Power Electron.*, Vol. 21, No. 1, pp. 193-201, Jan. 2006.
[18] Z. Zou, K. Zhou, Z. Wang, and M. Cheng, "Frequency-adaptive fractional-order repetitive control of shunt active power filters," *IEEE Trans. Ind. Electron.*, Vol. 62, No. 3, pp. 1659-1668, Apr. 2015.
[19] D. P. Estevez, J. D. Gandoy, A. G. Yepes, O. Yopez, and F. Baneira, "Enhanced resonant current controller for grid-connected converters with LCL filter," *IEEE Trans. Power Electron.*, Vol. 33, No. 5, pp. 3765-3778, May 2018.
[20] J. Dannehl, F W Fuchs and P. B. Thogersen, "PI state space current control of grid-connected PWM converters with LCL filters," *IEEE Trans. Power Electron.*, Vol. 25, No. 9, pp. 2320-2330, Sep. 2010.

Qingsong Wang was born in China, in 1982. He received his B.S. and M.S. degrees from the Department of Electrical Engineering, Zhejiang University, Hangzhou, China, in 2004 and 2007, respectively. He received his Ph.D. degree from the School of Electrical Engineering, Southeast University, Nanjing, China, in 2016. From November 2015 to November 2016, he was a joint Ph.D. student with the Department of Energy Technology, Aalborg University, Aalborg, Denmark, where his research focused on the control of electric springs. From July 2004 to July 2005, he was an Engineer in the Shihlin Electronic & Engineering Co., Ltd., Suzhou, China. From July 2007 to August 2011, he was an Engineer in the Global Development Center of Philips Lighting Electronics, Shanghai, China. In October 2010, he was promoted to Senior Engineer. From August 2011 to September 2013, he was a Lecturer in the PLA University of Science and Technology, Nanjing, China. Since 2017, he has been with Southeast University, where he is presently working as a Lecturer in the School of Electrical Engineering. Dr. Wang is a Senior Member of IEEE. His current research interests include the control and application of power electronics to microgrids, electric springs and distributed energy storage.

Wujian Zuo was born in China, in 1992. He received his B.S. degree from the School of Electrical Engineering and Control Science, Nanjing Tech University, Nanjing, China, in 2016. He is presently working towards his M.S. degree in the School of Electrical Engineering, Southeast University, Nanjing, China, where he is focused on the control of electric springs. His current research interests include the application of power electronics to power systems.

Ming Cheng was born in China, in 1960. He received his B.S. and M.S. degrees in Electrical Engineering from the Department of Electrical Engineering, Southeast University, Nanjing, China, in 1982 and 1987, respectively. He received his Ph.D. degree from the Department of Electrical and Electronic Engineering, University of Hong Kong, Hong Kong SAR, China, in 2001. Since 1987, he has been with Southeast University, where he is presently working as a Distinguished Professor in the School of Electrical Engineering and as the Director of the Research Center for Wind Power Generation. From January to April 2011, he was a Visiting Professor in the Wisconsin Electric Machine and Power Electronics Consortium, University of Wisconsin, Madison WI, USA. His current research interests include electrical machines, motor drives for electric vehicles, and renewable energy generation. He has authored or coauthored over 350 technical papers and four books. He is also the holder of 90 patents. Professor Cheng is a Fellow of the Institution of Engineering and Technology. He has served as a Chair and Organizing Committee Member for many international conferences. He was a Distinguished Lecturer of the IEEE Industry Applications Society (IAS) in 2015/2016.

Fujin Deng was born in China, in 1983. He received his B.S. degree in Electrical Engineering from the China University of Mining and Technology, Jiangsu, China, in 2005; his M.S. degree in Electrical Engineering from Shanghai Jiao Tong University, Shanghai, China, in 2008; and his Ph.D. degree in Energy Technology from the Department of Energy Technology, Aalborg University, Aalborg, Denmark, in 2012. In 2017, he joined Southeast University, Nanjing, China, where he is presently working as a Professor in the School of Electrical Engineering. From 2013 to 2015, he was a Postdoctoral Researcher, and from 2015 to 2017, he was an Assistant Professor in the Department of Energy Technology, Aalborg University. His current research interests include wind power generation, multilevel converters, high-voltage direct-current technology, DC grids, and offshore wind farm-power system dynamics.

Giuseppe Buja was born in Padova, Italy. He received his "Laurea" degree with honors in Power Electronics Engineering from the University of Padova, Padova, Italy, where he is presently working as a Full Professor. He has carried out extensive research work in the field of power and industrial electronics. His current research interests include automotive electrification, including the wireless charging of electric vehicles, and the grid-integration of renewable energies. Dr. Buja received an IEEE Industrial Electronics Society (IES) Eugene Mittelmann Achievement Award "in recognition of his outstanding technical contributions to the field of industrial electronics," and a 2016 Best Paper Award from the IEEE Transactions on Industrial Electronics. He has served the IEEE in several capacities, including General Chairman of the 20th Annual Conference of the IES (IECON) in 1994. He is presently an Associate Editor of the IEEE Transactions on Industrial Electronics, a Member of the Editorial Board of the Chinese Journal of Electrical Engineering, and a Senior Member of the Administrative Committee of the IES.